

# Multistage Reversible $T_g$ Photo-Modulation and Hardening of Hydrazone-Containing Polymers

Sirun Yang,<sup>†</sup> Jared D. Harris,<sup>†</sup> Aloshious Lambai,<sup>‡</sup> Laura L. Jeliaskov,<sup>†</sup> Gaurav Mohanty,<sup>‡</sup> Hao Zeng,<sup>‡</sup> Arri Priimagi,<sup>‡</sup> and Ivan Aprahamian<sup>†\*</sup>

<sup>†</sup> Department of Chemistry, Dartmouth College, Hanover, New Hampshire 03755, United States

<sup>‡</sup> Faculty of Engineering and Natural Sciences, Tampere University, Korkeakoulunkatu 10, Tampere, 33720 Finland

*Glass transition, polymer, hydrazone, photoswitch, photo-hardening*

---

**ABSTRACT:** A series of poly(methyl acrylate)- and poly(methyl methacrylate)-based polymers containing bistable hydrazone photoswitch pendants were synthesized by reversible addition-fragmentation chain-transfer polymerization. An increase in the polymers' glass transition temperature ( $T_g$ ) was observed upon  $Z \rightarrow E$  photoisomerization, resulting in the photo-hardening of the polymeric network. This effect was corroborated using nanoindentation measurements that show increase in hardness (18%) and modulus (7.5%) upon photoswitching. The bistability of the switch allowed for the indefinite locking-in of the properties of the  $E$ -rich polymer at ambient temperature. Moreover, and unlike in other photoswitchable polymers, the photo engineered  $T_g$  was sustained even at elevated temperatures of up to 150 °C. This unique property allowed us to dial-in multiple  $T_g$  values in the same polymeric material as a function of the hydrazones switch's  $Z/E$  isomer ratio, which is unprecedented. The reported strategy presents a new opportunity for the post-synthetic photo-tuning of the physical properties of polymers.

---

The temperature at which a polymer transitions from a hard and glassy state into a soft rubbery one is termed the glass transition temperature ( $T_g$ ). This physical property defines the mechanical characteristics of a polymer, how it can be applied, and whether it is re-processable and healable at ambient temperatures.<sup>1,2</sup> In most cases the  $T_g$  of a polymer, and hence its associated properties, is difficult to change once the polymer is made. Post-synthetic modification of  $T_g$  values typically requires the addition of plasticizers, which, while cheap and effective in reducing the  $T_g$ , may compromise other physical properties of the material, reduce its shelf-life, and cause pollution.<sup>3,4</sup> Alternatively, photo-melting,<sup>5-10</sup> induced by the *trans/cis* isomerization of azobenzene,<sup>11</sup> can be used to change the  $T_g$  value, though this process is far less explored and understood. This strategy is promising for post-synthetic polymer property engineering, and having a better understanding and control over it will result in various applications in photolithography, self-healable devices, actuators, etc.<sup>5-10, 12 - 16</sup> However, there exists a significant drawback in this approach as the metastability of the *cis* form of azobenzene prevents effective locking-in of the photo-engineered  $T_g$  values, and hence, properties.<sup>5-10,17</sup>

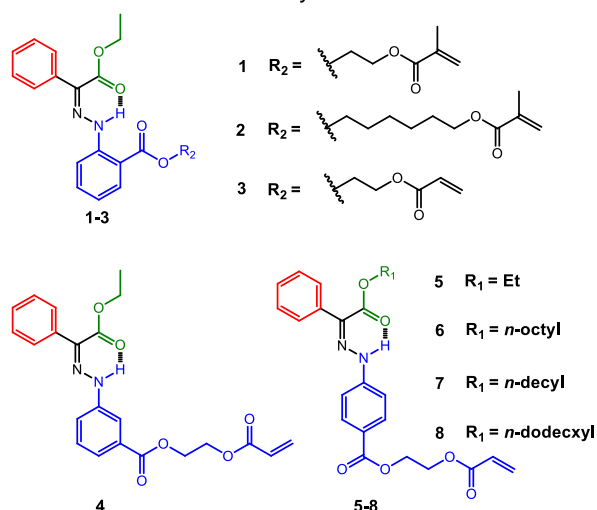
We recently reported on a new family of bistable photochromic hydrazones<sup>18-24</sup> having thermal isomerization (*i.e.*,  $E \rightarrow Z$ ) half-lives of thousands of years.<sup>19</sup> This unusual property in the context of configurational switches was

subsequently used in the kinetic trapping of i) different shapes of a liquid-crystalline elastomer strip,<sup>25</sup> and ii) self-assembled helical structures of liquid crystals,<sup>26</sup> and hence their photophysical properties. In both cases, the hydrazone switching resulted in a novel order-to-order transition in the bulk system (vs. the order-to-disorder transition observed in azobenzene-based systems<sup>27-36</sup>). We postulated that the bistability of the hydrazones combined with the order-to-order transition they induce would allow us to design and lock-in innovative polymeric functions and properties that are not possible with the photochromic compounds currently in the literature, especially azobenzene.

Herein, we verify this hypothesis by incorporating the hydrazone photoswitches into polyacrylate- and polymethacrylate-based polymers as side chains and studied how photoisomerization and nature of the polymer affect the  $T_g$  value and difference in  $T_g$  value ( $\Delta T_g$ ) upon isomerization. We show that the photoswitching results in photo-hardening of the polymers, *i.e.*, the  $T_g$  value increases as a function of light irradiation, as opposed to the photo-melting. We ascribe this result to the order-to-order transition that hydrazones induce in bulk material, allowing for stronger interactions between the polymer chains. This behavior is similar to what is observed in heat-stiffening polymer composites.<sup>37-39</sup> We also carried structure property analysis to lower the initial  $T_g$  value to ambient and

physiologically relevant temperatures to enable their future use in 3D printing<sup>40</sup> or bioimplants.<sup>41</sup> The end goal here is the development of polymers that can be induced to undergo liquid-to-solid phase transitions, with properties that can be precisely controlled and dialed-in. Finally, the bistability of the hydrazone switches allowed us to lock-in different  $T_g$  values for the same polymer as a function of irradiation wavelength, *i.e.*, the  $Z/E$  isomer ratio at the photostationary state (PSS), a feat that has not been accomplished before. This photo-hardening strategy presents a new avenue for the post-synthetic manipulation of adaptable, healable,<sup>3-4</sup> and shape-memory<sup>42,43</sup> polymers among other applications.<sup>5-10</sup>

#### a) Monomers used in this Study



#### b) Polymer Synthesis

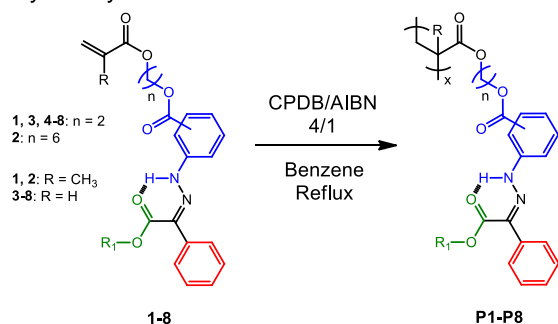


**Figure 1.** a) The monomers (**1-8**) used in this study; and b) Synthesis of polymers **P1-P8** via reversible addition-fragmentation chain-transfer polymerization.

The hydrazone monomers **1-8** (Figure 1a) were synthesized in 57-87% yield by following earlier established protocols (Scheme S1 and S3).<sup>25</sup> The hydrazones were characterized using NMR spectroscopy (Figure S2-S17) and ESI mass spectroscopy. The monomers were then (Figure 1b) subjected to reversible addition-fragmentation chain-transfer polymerization conditions with a target degree of polymerization of 150 to give polymers **P1-P8** in reasonable yields (41-85%). The polymers were characterized using <sup>1</sup>H NMR spectroscopy (Figure S18-S25), and their molecular weights (Figure S1 and Table S1) determined using gel permeation chromatography. The photoswitching properties of the polymers, namely their  $Z/E$  isomerization,

in both solution and as thin films, were investigated by UV/vis spectroscopy (Figures S42-S57), and their PSSs at particular wavelengths were determined using <sup>1</sup>H NMR spectroscopy. In general, a solution of  $Z$ -enriched polymer (pristine state, >99 %  $Z$ ) in  $\text{CD}_2\text{Cl}_2$  was irradiated with 410 nm light until the photostationary state (PSS<sub>410</sub>) was reached. The PSS<sub>410</sub> consisted of >94 % of the  $E$  isomer as observed by <sup>1</sup>H NMR spectroscopy. Back-isomerization from the  $E$  to  $Z$  isomer was achieved by irradiation of an  $E$ -enriched solution with 340 nm light to yield 68-83% of the  $Z$  isomer (Figures S58-S64 and S92). The switching cycle of **P5** (Figure 2a) is given here as an example: the pristine polymer has a maximum absorption ( $\lambda_{\text{max}}$ ) at 368 nm, which shifts to 338 nm (Figure 2b) upon irradiation with 410 nm light (PSS<sub>410</sub> consisting of 97%  $E$  isomer (Figure S83)). The reverse process is induced by irradiation of the  $E$ -enriched sample with 340 nm light, resulting in a red shift of the  $\lambda_{\text{max}}$  to 364 nm, and a PSS<sub>340</sub> consisting of 83%  $Z$  isomer.

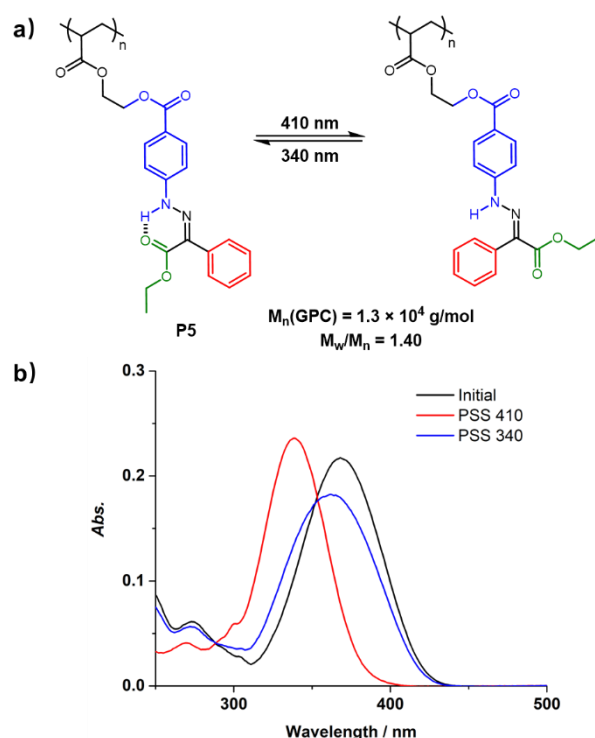


**Figure 2.** a) Light-activated photoisomerization of **P5**; and b) its UV/Vis spectra in  $\text{CH}_2\text{Cl}_2$  (4  $\mu\text{g/mL}$ ) before (black) and after irradiation with 410 nm light (red), followed by irradiation with 340 nm light (blue).

The  $T_g$  values (Table 1), determined from second heating of the polymers, were measured using a heat/cool/heat program cycling (35 $\rightarrow$ 150 $\rightarrow$ 0 $\rightarrow$ 150  $^\circ\text{C}$ ) at a rate of 10  $^\circ\text{C min}^{-1}$ . Samples ( $\sim$  6-10 mg) were prepared in aluminum Tzero pans and were either pristine precipitates (>99 %  $Z$  by <sup>1</sup>H NMR) or  $E$ -enriched (*via* irradiation to PSS). For more details, please see the Supporting Information.

The modularity of the hydrazones enabled us to use structure property analysis to assess how substitution patterns and length of alkyl linkers modulate the  $T_g$  and  $\Delta T_g$  values (Table 1). We started the study with the polymethacrylate polymers **P1** and **P2**. Polymer **P1** has a pristine  $T_g$  of

86 °C which increases to 103 °C upon photoisomerization to an *E*-enriched state, resulting in a  $\Delta T_g$  of 17 °C. Polymer **P2** has a pristine  $T_g$  of 41 °C and a  $\Delta T_g$  of 7 °C, indicating that the lengthening of the alkyl tether attaching the hydrazone to the polymer backbone enhances the free volume in the polymer (lowering  $T_g$ ) while mitigating the change in free volume upon photoisomerization (lowering  $\Delta T_g$ ). This result suggests that achieving large  $\Delta T_g$  requires the photoswitch to be in relatively close proximity to the polymer backbone. These preliminary results were considered in the development of hydrazone polymers **P3-P8**. The objectives with the design of these polymers were to i) lower the initial  $T_g$  value to ambient temperatures, and ii) maximize the  $\Delta T_g$  value to achieve a wider range of  $T_g$  tunability.

**Table 1. Summary of the  $T_g$ 's of P1-P8 before and after isomerization**

Polymer	$T_g$ Pristine (°C) (Z > 99 %)	$T_g$ PSS <sub>410</sub> (°C) (E %)	$\Delta T_g$ (°C) <sup>a</sup>
<b>P1</b>	86	103 (94 %)	+17
<b>P2</b>	41	48 (95 %)	+7
<b>P3</b>	68	79 (95 %)	+11
<b>P4</b>	64	73 (98 %)	+9
<b>P5</b>	75	97 (97 %)	+22
<b>P6</b>	28	42 (98 %)	+14
<b>P7</b>	20	35 (98 %)	+15
<b>P8</b>	21	37 (98 %)	+16

a.  $\Delta T_g = T_g \text{ PSS}_{410} - T_g \text{ pristine}$

With these goals in mind, we switched to a polyacrylate backbone, which inherently has a lower  $T_g$  than its polymethacrylate counterpart. **P3** was designed as the polyacrylate equivalent of **P1**, and as expected it has lower pristine and switched (i.e., *E*-enriched)  $T_g$  values (68 and 79 °C, respectively). It also, however, has a slightly lower  $\Delta T_g$  value of 11 °C as opposed to 17 °C for **P1**, indicating that the change in free volume is smaller upon switching. To address this issue and study the effect of the substitution pattern on the polymer properties, we synthesized polymers **P4** and **P5**, which have the acrylate group attached at the *meta* and *para* positions of the stator phenyl group (blue, Figure 1a), respectively, instead of the *ortho* one as in **P1/P3**. **P4** yielded a smaller  $\Delta T_g$  value (9 °C) than **P1**, while **P5** yielded the large  $\Delta T_g$  value (22 °C) in the whole series. These results indicate that pristine **P5**, which also has the highest  $T_g$  value in the acrylate series, has the best molecular packing among the three substitution positions in both pristine and irradiated states.

We retained the *para* substitution pattern in our next designs and moved our focus to lowering the overall  $T_g$  value near to ambient temperature. We hypothesized that

extending the alkyl chain length attached to the rotor ester group (green, Figure 1a) would add free volume to the polymer, thus lowering the  $T_g$ . Hence, polymers **P6 - P8** were synthesized having octyl, decyl and dodecyl chains attached to the ester group, respectively. This design motif successfully lowered the  $T_g$  values of the polymers to the range of 20 to 42 °C (Table 1). Moreover, a relatively large  $\Delta T_g$  value was consistently maintained ( $\Delta T_g \approx +15$  °C) in all three polymers. The difference in  $T_g$  of **P7** and **P8** was minimal indicating that we reached the limit of the extended alkyl group approach. More importantly the pristine  $T_g$  values of **P6-P8** are now at ambient and even physiologically relevant temperatures, indicating that our structure property analysis driven approach for tuning the  $T_g$  and  $\Delta T_g$  values was successful.

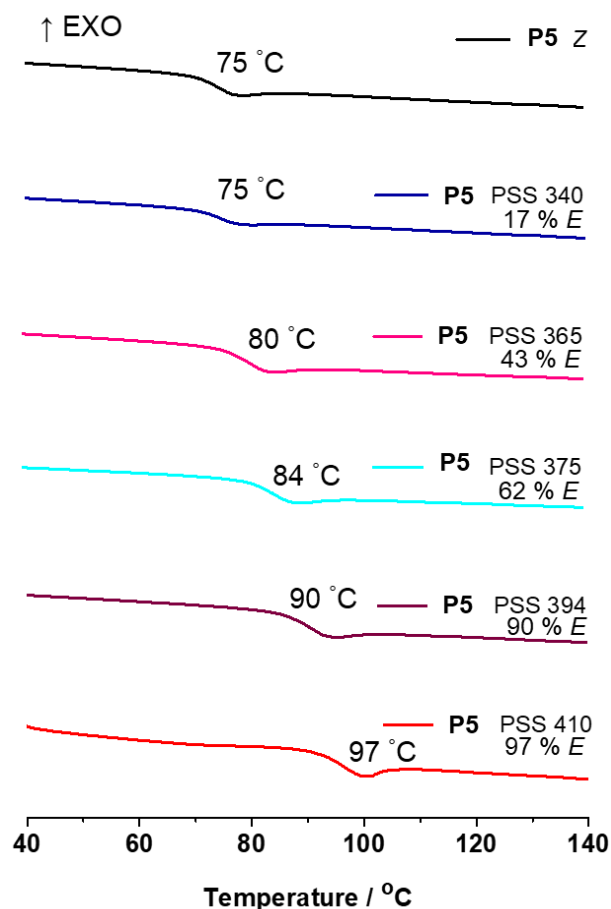


**Figure 3.** Second cycle DSC curves at the different PSSs of **P5** as obtained by irradiation using wavelengths of light between 340 and 410 nm.

To take full advantage of the intrinsic bistability of the hydrazones, we demonstrated that the  $T_g$  of the polymers can be manipulated not only in a binary manner between the *Z* and *E* forms, but also incrementally as a function of wavelength-dependent PSS, i.e., isomer ratio. We decided to use **P5** for this demonstration as it has the largest  $\Delta T_g$  value. As can be seen in Figure 3 various  $T_g$  values between 75 and 97 °C can be locked in by controlling the PSS. The *Z/E* isomer ratios at the different PSS values were measured using <sup>1</sup>H NMR spectroscopy after irradiation with 340, 365, 375, 394, and 410 nm light. Moving from PSS<sub>365</sub> to

PSS<sub>410</sub> steps of 4–7 °C difference in  $T_g$  values are obtained, which correspond to the increase in the *E* isomer ratio in the polymer. Moreover, the lack of a difference between the first and second heating cycle traces in the DSC measurements confirms that each of these  $T_g$  values can be locked in place (Figure 3). This premise is true even at temperatures as high as 150 °C as no exothermic peak,<sup>6,17</sup> which is indicative of *E*→*Z* thermal isomerization is observed during the heating cycles (Figure S93). This observation confirms the stability of the *E* isomer within the temperature bounds evaluated and demonstrates the benefit of using bistable hydrazone photoswitches in controlling the  $T_g$  values of polymers.<sup>17</sup>

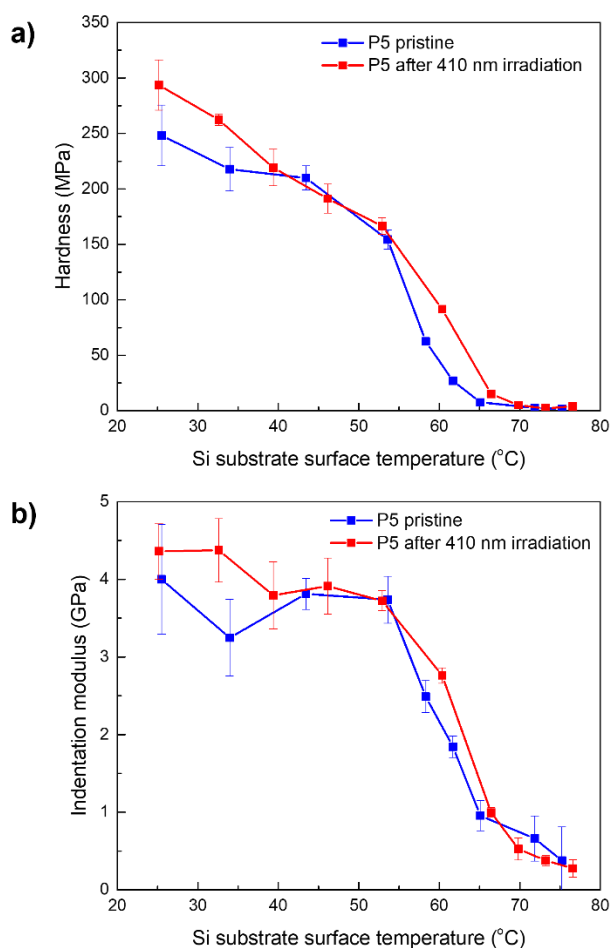


**Figure 4.** a) Indentation hardness and b) modulus **P5** before and after 410 nm irradiation.

Finally, to verify the improved molecular packing upon *Z*→*E* photoisomerization,<sup>44</sup> we performed variable-temperature nanoindentation studies<sup>45</sup> to investigate the photo-induced changes in the hardness and modulus of the hydrazone polymers (Figure 4; Details are in the Supporting Information). Alike to the gradual  $T_g$  control experiments (Figure 3), **P5** was our polymer of choice for this experiment, rationalized by its large  $\Delta T_g$  value. Because of the difficulty in measuring the polymer film surface temperature accurately, the temperature of the silicon substrate onto which the films were deposited on has been reported instead. At room temperature, the hardness increases from 248 to 294 MPa, *i.e.*, by 18 %, upon light irradiation. At increased temperature, the hardness systematically

decreases and becomes immeasurable once the  $T_g$  is reached. While the photo-hardening is more difficult to detect at elevated temperatures, the general trend seems to prevail (Figure 4a). The light-induced change in modulus (from 4 GPa to 4.4 GPa) is less drastic (7.5%) than the change in hardness. We hypothesize that this stems from the elastic influence of the underlying non-photoswitched material within the 30  $\mu\text{m}$  thick polymer film used in these experiments, of which only the top layer can be converted to an *E*-rich PSS. The indentation modulus is more severely influenced by the non-photoconverted film fraction in comparison to hardness for equivalent indentation depths for graded materials and thin films.<sup>46</sup> The nanoindentation results further pinpoint the unique role the bistable hydrazone photoswitches play in the photochemical control over the thermomechanical properties of polymers: both azobenzene-containing amorphous polymers<sup>47-49</sup> and liquid crystalline polymer networks<sup>50-52</sup> typically soften upon photoirradiation. Moreover, in these examples, the *cis*-state of azobenzene prevails for hours at most and in the case of fast-switching azobenzenes, photothermal heating is likely to contribute to the photo-softening. Hence the lock-in of the photoinduced changes, as reported here, is unachievable with azobenzenes.

In conclusion, a correlation between *Z*/*E* isomer ratio and  $T_g$  value was observed in a series of polyacrylate- and polymethacrylate-based polymers having bistable hydrazone photoswitches as pendants. As the amount of *E* isomer propagates in the polymer, an obvious increase in  $T_g$  – up to 22 °C – is observed. We attribute this observation to an increase in order that the hydrazones induce upon *Z*→*E* photoisomerization, resulting in hitherto unreported photo-hardening effect. Variable-temperature nanoindentation studies show that this effect is taking place on the surface of the bulk material. The bistability of the hydrazones allows for the dialing-in and locking-in of various  $T_g$  values as a function of *E* isomer ratio even after several heating cycles. Further analysis of these effects will be geared towards testing whether this behavior can be extended to tuning the physical (*e.g.*, density)<sup>25</sup>, or thermal (*e.g.*, thermal conductivity)<sup>53</sup> properties of polymer.

## ASSOCIATED CONTENT

**Supporting Information.** General methods, experimental procedures, NMR spectra, photoisomerization and kinetic studies, DSC measurements. (PDF)

This material is available free of charge via the Internet at <http://pubs.acs.org>

## AUTHOR INFORMATION

Corresponding Author

**Ivan Aprahamian** – Department of Chemistry, Dartmouth College, Hanover, New Hampshire 03755, United States  
Email: [ivan.aprahamian@dartmouth.edu](mailto:ivan.aprahamian@dartmouth.edu)

Authors

**Sirun Yang** – Department of Chemistry, Dartmouth College, Hanover, New Hampshire 03755, United States

**Jared D. Harris** – Department of Chemistry, Dartmouth College, Hanover, New Hampshire 03755, United States

**Aloshious Lambai** – Faculty of Engineering and Natural Sciences, Tampere University, Korkeakoulunkatu 10, Tampere, 33720 Finland

**Laura L. Jeliaskov** – Department of Chemistry, Dartmouth College, Hanover, New Hampshire 03755, United States

**Gaurav Mohanty** – Faculty of Engineering and Natural Sciences, Tampere University, Korkeakoulunkatu 10, Tampere, 33720 Finland

**Hao Zeng** – Faculty of Engineering and Natural Sciences, Tampere University, Korkeakoulunkatu 10, Tampere, 33720 Finland

**Arri Priimagi** – Faculty of Engineering and Natural Sciences, Tampere University, Korkeakoulunkatu 10, Tampere, 33720 Finland

## Notes

The authors declare no competing financial interest.

## ACKNOWLEDGMENT

I.A. is grateful to the NSF (CHE-1807428) for the generous support. J.D.H. thanks the Dartmouth College Society of Fellows for their generous support. This work has been supported by the Academy of Finland Flagship Programme, Photonics Research and Innovation, Decision Number 321065. The work is partially conducted in the premises of Tampere Microscopy Center, which is gratefully acknowledged.

## REFERENCES

- (1) Colquhoun, H. M. Materials that heal themselves. *Nat. Chem.* **2012**, *4*, 435–436.
- (2) Yang, Y.; Urban, M. W. Self-healing polymeric materials. *Chem. Soc. Rev.* **2013**, *42*, 7446–7467.
- (3) Bergman, S.D.; Wudl, F. Mendable polymers. *J. Mater. Chem.* **2008**, *18*, 41–62.
- (4) Fiore, G. L.; Rowan, S. J.; Weder, C. Optically healable polymers. *Chem. Soc. Rev.* **2013**, *42*, 7278–7288.
- (5) Brown, E.; Rodenberg, N.; Amend, J.; Mozeika, A.; Steltz, E.; Zakin, M.R.; Lipson, H.; Jaeger, H.M. Universal robotic gripper based on the jamming of granular material. *Proc. Natl. Acad. Sci. U. S. A.* **2010**, *107*, 18809–18814.
- (6) Zhou, H.; Xue, C.; Weis, P.; Suzuki, Y.; Huang, S.; Koynov, K.; Auernhammer, G. K.; Berger, R.; Butt, H.; Wu, S. Photoswitching of glass transition temperatures of azobenzene-containing polymers induces reversible solid-to-liquid transitions. *Nat. Chem.* **2017**, *9*, 145–151.
- (7) Weis, P.; Tian, W.; Wu, S. Photoinduced Liquefaction of Azobenzene-Containing Polymers. *Chem. Eur. J.* **2018**, *24*, 6494–6505.
- (8) Narang, Y.S.; Degirmenci, A.; Vlassak, J.J.; Howe, R.D. Transforming the dynamic response of robotic structures and systems through laminar jamming. *IEEE Robot. Autom. Lett.* **2018**, *3*, 688–695.
- (9) Wu, S. Photoinduced Reversible Solid-to-Liquid Transitions for Photoswitchable Materials. *Angew. Chem. Int. Ed.* **2019**, *58*, 9712–9740.
- (10) Linghu, C.; Zhang, S.; Wang, C.; Yu, K.; Li, C.; Zeng, Y.; Zhu, H.; Jin, X.; You, Z.; Song, J. Universal SMP gripper with massive and selective capabilities for multiscaled, arbitrarily shaped objects. *Sci. Adv.* **2020**, *6*, eaay5120.
- (11) Bandara, H. D.; Burdette, S. C. Photoisomerization in different classes of azobenzene. *Chem. Soc. Rev.* **2012**, *41*, 1809–1825.
- (12) Karageorgiev, P.; Neher, D.; Schulz, B.; Stiller, B.; Pietsch, U.; Giersig, M.; Brehmer, L. From anisotropic photo-fluidity towards nanomanipulation in the optical near-field. *Nat. Mater.* **2005**, *4*, 699–703.
- (13) Lee, S.; Kang, H. S.; Park, J.-K. Directional Photofluidization Lithography: Micro/Nanostructural Evolution by Photofluidic Motions of Azobenzene Materials. *Adv. Mater.* **2012**, *24*, 2069–2103.
- (14) Yue, Y.; Norikane, Y.; Azumi, R.; Koyama, E. Light-Induced Mechanical Response in Crosslinked Liquid-Crystalline Polymers with Photoswitchable Glass Transition Temperatures. *Nat. Commun.* **2018**, *9*, 3234.
- (15) Ito, S.; Akiyama, H.; Mori, M.; Yoshida, M.; Kihara, H. Azobenzene-Containing Triblock Copolymer Adhesive Based on Light-Induced Solid-Liquid Phase Transition: Application to Bonding for Various Substrates. *Macromol. Chem. Phys.* **2019**, *220*, 1900105.
- (16) Uchida, E.; Azumi, R.; Norikane, Y. Light-induced crawling of crystals on a glass surface. *Nat. Commun.* **2015**, *6*, 7310.
- (17) Appiah, C.; Woltersdorf, G.; Pérez-Camargo, R. A.; Mglter, A. J.; Binder, W. H. Crystallization Behavior of Precision Polymers Containing Azobenzene Defects. *Eur. Polym. J.* **2017**, *97*, 299–307.
- (18) Su, X.; Lessing, T.; Aprahamian, I. The Importance of the Rotor in Hydrazone-Based Molecular Switches. *Beilstein J. Org. Chem.* **2012**, *8*, 872–876.
- (19) Qian, H.; Pramanic, S.; Aprahamian, I. Photochromic Hydrazone Switches with Extremely Long Thermal Half-Lives. *J. Am. Chem. Soc.* **2017**, *139*, 9140–9143.
- (20) Shao, B.; Qian, H.; Li, Q.; Aprahamian, I. Structure Property Analysis of the Solution and Solid-State Properties of Bistable Photochromic Hydrazones. *J. Am. Chem. Soc.* **2019**, *141*, 8364–8371.
- (21) Zheng, L.-Q.; Yang, S.; Lan, J.; Gyr, L.; Goubert, G.; Qian, H.; Aprahamian, I.; Zenobi, R. Solution phase and surface photoisomerization of a hydrazone switch with long thermal half-life. *J. Am. Chem. Soc.* **2019**, *141*, 17637–17645.
- (22) Guo, X.; Shao, B.; Zhou, S.; Aprahamian, I.; Chen, Z. Visualizing intracellular particles and precise control of drug release using an emissive hydrazone photochrome. *Chem. Sci.* **2020**, *11*, 3016–3021.
- (23) Shao, B.; Aprahamian, I. Hydrazones as New Molecular Tools. *Chem* **2020**, *6*, 2162–2173.
- (24) Yang, S.; Larsen, D.; Pellegrini, M.; Meier, S.; Mierke, D. F.; Beeren, S. R.; Aprahamian, I. Dynamic enzymatic synthesis of  $\gamma$ -cyclodextrin using a photoremovable hydrazone template. *Chem* **2021**, *7*, 2190–2200.
- (25) Ryabchun, A.; Li, Q.; Lancia, F.; Aprahamian, I.; Katsonis, N. Shape-persistent actuators from hydrazone photoswitches. *J. Am. Chem. Soc.* **2019**, *141*, 1196–1200.
- (26) Moran, M. J.; Magrini, M.; Walba, D. M.; Aprahamian, I. Driving a liquid crystal phase transition using a photochromic hydrazone. *J. Am. Chem. Soc.* **2018**, *140*, 13623–13627.
- (27) Ikeda, T.; Tsutsumi, O. Optical switching and image storage by means of azobenzene liquid-crystal films. *Science* **1995**, *268*, 1873–1875.
- (28) Ikeda, T. Photomodulation of liquid crystal orientations for photonic applications. *J. Mater. Chem.* **2003**, *13*, 2037–2057.
- (29) Wang, Y.; Urbas, A.; Li, Q. Reversible Visible-Light Tuning of Self-Organized Helical Superstructures Enabled by Unprecedented Light-Driven Axially Chiral Molecular Switches. *J. Am. Chem. Soc.* **2012**, *134*, 3342–3345.
- (30) Kim, Y.; Tamaoki, N. A photoresponsive planar chiral azobenzene dopant with high helical twisting power. *J. Mater. Chem. C* **2014**, *2*, 9258–9264.
- (31) Kim, Y.; Tamaoki, N. Asymmetric dimers of chiral azobenzene dopants exhibiting unusual helical twisting power upon photoswitching in cholesteric liquid crystals. *ACS Appl. Mater. Interfaces* **2016**, *8*, 4918–4926.



(32) Bisoyi, H. K.; Li, Q. Light-driven liquid crystalline materials: from photo-induced phase transitions and property modulations to applications. *Chem. Rev.* **2016**, *116*, 15089–15166.

(33) Nishikawa, H.; Mochizuki, D.; Higuchi, H.; Okumura, Y.; Kikuchi, H. Reversible Broad-Spectrum Control of Selective Reflections of Chiral Nematic Phases by Closed-/Open-Type Axially Chiral Azo Dopants. *ChemistryOpen* **2017**, *6*, 710–720.

(34) Wang, L.; Chen, D.; Gutierrez-Cuevas, K. G.; Bisoyi, H. K.; Fan, J.; Zola, R. S.; Li, G.; Urbas, A. M.; Bunning, T. J.; Weitz, D. A.; Li, Q. Optically reconfigurable chiral microspheres of self-organized helical superstructures with handedness inversion. *Mater. Horiz.* **2017**, *4*, 1190–1195.

(35) Wang, H.; Bisoyi, H. K.; Wang, L.; Urbas, A. M.; Bunning, T.; Li, Q. Photochemically and Thermally Driven Full-Color Reflection in a Self-Organized Helical Superstructure Enabled by a Halogen-Bonded Chiral Molecular Switch. *Angew. Chem., Int. Ed.* **2018**, *57*, 1627–1631.

(36) Huang, H.; Orlova, T.; Matt, B.; Katsonis, N. Long-Lived Supramolecular Helices Promoted by Fluorinated Photoswitches. *Macromol. Rapid Commun.* **2018**, *39*, 1700387.

(37) Hsu, L.; Weder, C.; Rowan, S. J. Stimuli-Responsive, Mechanically-Adaptive Polymer Nanocomposites. *J. Mater. Chem.* **2011**, *21*, 2812–2822.

(38) Pérez-Madrigal, M.M.; O'Reilly, R.K. Thermally switching on/off the hardening of soaked nanocomposite materials. *ACS Cent. Sci.* **2017**, *3*, 817–819.

(39) Cudjoe, E.; Khani, S.; Way, A.E.; Hore, M.J.; Maia, J.; Rowan, S.J. Biomimetic reversible heat-stiffening polymer nanocomposites. *ACS Cent. Sci.* **2017**, *3*, 886–894.

(40) Gastaldi, M.; Cardano, F.; Zanetti, M.; Viscardi, G.; Barolo, C.; Bordiga, S.; Magdassi, S.; Fin, A.; Roppolo, I. Functional Dyes in Polymeric 3D Printing: Applications and Perspectives. *ACS Materials Lett.* **2021**, *3*, 1–17.

(41) Cheekuramelli, N. S.; Late, D.; Kiran, S.; Garnaik, B. Biodegradable and Biocompatible Polymer Composite. In *Lightweight Polymer Composite Structures*; CRC Press: Boca Raton, FL, 2020; pp 67–88.

(42) Miaudet, P.; Derre, A.; Maugey, M.; Zakri, C.; Piccione, P.M.; Inoubli, R. Poulin, P. Shape and Temperature Memory of Nanocomposites with Broadened Glass Transition. *Science* **2007**, *318*, 1294–1296.

(43) Xie, T.; Rousseau, I.A. Facile Tailoring of Thermal Transition Temperatures of Epoxy Shape Memory Polymers. *Polymer*, **2009**, *50*, 1852–1856.

(44) Wang, G.; Zhang, Q.; Zhu, F.; Zhang, C.; Li, H.; Lu, J. Controllable Binary/Ternary Memory Behavior Induced by Isomerization of Phenylhydrazone Groups in Polymer Side Chains Under Ultraviolet Light Conditions. *J. Mater. Chem. C* **2021**, *9*, 6351–6356.

(45) Conte, M.; Mohanty, G.; Schwiedrzik, J. J.; Wheeler, J. M.; Bellaton, B.; Michler, J.; Randall, N. X. Novel high temperature vacuum nanoindentation system with active surface referencing and non-contact heating for measurements up to 800 °C. *Rev. Sci. Instrum.* **2019**, *90*, 045105.

(46) Saha, R.; Nix, W. D. Effects of the substrate on the determination of thin film mechanical properties by nanoindentation. *Acta Mater.* **2002**, *50*, 23–38.

(47) Srihirin, T.; Laschitsch, A.; Neher, D.; Johannsmann, D. Light-induced softening of azobenzene dye-doped polymer films probed with quartz crystal resonators. *Appl. Phys. Lett.* **2000**, *77*, 963–965.

(48) Kim, H. K.; Wang, X. S.; Fujita, Y.; Sudo, A.; Nishida, H.; Fujii, M.; Endo, T. Reversible photo-mechanical switching behavior of azobenzene-containing semi-interpenetrating network under UV and visible light irradiation. *Macromol. Chem. Phys.* **2005**, *206*, 2106–2111.

(49) Vapaavuori, J.; Mahimwalla, Z.; Chromik, R.R.; Kaivola, M.; Priimagi, A.; Barrett, C. J. Nanoindentation study of light-induced softening of supramolecular and covalently functionalized azo polymers. *J. Mater. Chem. C* **2013**, *1*, 2806–2810.

(50) Shimamura, A.; Priimagi, A.; Mamiya, J.I.; Ikeda, T.; Yu, Y.; Barrett, C.J.; Shishido, A. Simultaneous analysis of optical and mechanical properties of cross-linked azobenzene-containing liquid-crystalline polymer films. *ACS Appl. Mater. Interfaces* **2011**, *3*, 4190–4196.

(51) Kumar, K.; Schenning, A. P.; Broer, D. J.; Liu, D. Regulating the modulus of a chiral liquid crystal polymer network by light. *Soft Matter*, **2016**, *12*, 3196–3201.

(52) Lancia, F.; Ryabchun, A.; Nguindjel, A.D.; Kwangmettam, S.; Katsonis, N. Mechanical adaptability of artificial muscles from nanoscale molecular action. *Nat. Commun.* **2019**, *10*, 4819.

(53) Shin, J.; Sung, J.; Kang, M.; Xie, X.; Lee, B.; Lee, K. M.; White, T. J.; Leal, C.; Sottos, N.R.; Braun, P.V.; Cahill, D.G. Light-Triggered Thermal Conductivity Switching in Azobenzene Polymers. *Proc. Natl. Acad. Sci. U.S.A.* **2019**, *116*, 5973–5978.

